

ORIGINAL ARTICLE

Synergic Toxicity of Solid Particles and Released Zinc from Zinc Oxide Nanoparticles to Human Lung Epithelial Cells

Fei Zhuang¹, and Nobutaka Hanagata^{1,2}

¹*Graduate School of Life Science, Hokkaido University, Sapporo, Japan.*

²*Nanotechnology Innovation Station,
National Institute for Materials Science, Tsukuba, Japan.*

Synopsis

To identify the respective contributions of released zinc and solid particles on the cytotoxicity of zinc oxide nanoparticles (ZnO-NPs), we exposed A549 cells to ZnO-NP suspensions, their extractions collected after centrifugation, and medium containing zinc chloride (ZnCl₂). We then assayed the cytotoxicity of these samples using water-soluble tetrazolium salts (WSTs) and intracellular reactive oxygen species (ROS) with 2',7'-dichlorodihydrofluorescein diacetate (DCFH-DA) as outputs. Only the ZnO-NP suspension caused cytotoxicity and increased intracellular ROS; the extractions and ZnCl₂ did not cause cytotoxicity or oxidative stress. Global gene expression analysis revealed that both ZnCl₂-containing medium and the ZnO-NP suspension caused upregulation of the "cadmium binding" gene functional category. This category consisted of metallothioneins (MTs), important zinc-homeostasis proteins. To further investigate the role of MTs in ZnO-NP-dependent cytotoxicity, we inhibited the overexpression of MTs with corresponding siRNA and found that released zinc contributed to ZnO-NP-dependent cytotoxicity. We conclude that both solid particles and released zinc contributed to ZnO-NP-dependent cytotoxicity. Additionally, we propose a synergic relationship between ZnO-NPs and MTs.

Key words: *zinc oxide nanoparticles, synergic cytotoxicity, released zinc, metallothioneins, intracellular reactive oxygen species*

Introduction

Zinc oxide nanoparticles (ZnO-NPs) have been extensively applied in electronics, optoelectronics, gas sensors, sunscreens, and antibacterial coatings due to their unique properties arising from quantum confinement, including antibacterial, antifungal, and ultraviolet filtering properties, as well as high catalytic and photochemical activity [1-4]. However, epidemiological and *in vivo* studies have lagged behind the speed of mass ZnO-NP production, thereby escalating human exposure risks [5, 6]. Unfortunately, reports of ZnO-NP toxicity are becoming more

and more common, including reports of toxicity in aquatic organisms, terrestrial animals and plants, and microorganisms [7-10]. *In vitro* studies have also revealed that ZnO-NPs are toxic to various human cell lines, such as lung epithelial cells, aortic endothelial cells, epidermal cells, bronchial epithelial cells, lymphoblastoid cells, lung mesothelioma cells, and fibroblasts [11-18].

Currently, concerns have focused on whether the solid particles or the released zinc is the real toxicant in ZnO-NP-dependent cytotoxicity. On one hand, some findings have indicated

that solid particles play an important role. Moos *et al.* found that contact of particles with the cells was required for ZnO-NP-dependent cytotoxicity [14], while Gojova *et al.* concluded that the internalization of nanoparticles by the cells was necessary for ZnO-NP-induced cytotoxicity [13, 14]. Furthermore, ZnO-NP-dependent cytotoxicity was reported to result from increased intracellular reactive oxygen species (ROS) caused by the solid particles via a special interface chemical activity [12, 17, 19]. In contrast, Franklin *et al.* demonstrated the importance of the solubility of ZnO-NPs for toxicity in microalga [20]. Brunner also found that the solubility of ZnO-NPs was very important for cytotoxicity [18]. Additionally, another study suggested that the particles were internalized by the cells and intracellular released zinc was the true toxicant in ZnO-NP-induced cytotoxicity [21]. Xia and colleagues found accumulation of fluorescein isothiocyanate (FITC)-labeled ZnO-NPs in human bronchial epithelial cells and concluded the intracellular dissolution of these particles was important for their cytotoxicity [22]. However, Gojova *et al.* did not detect the uptake of ZnO-NPs, although they did find that the presence of solid particles was a prerequisite for their cytotoxicity [13, 14].

The objective of this study was to identify the respective contributions of solid particles and released zinc to ZnO-NP cytotoxicity. To this end, we prepared 3 types of exposure media: ZnO-NP suspensions in medium, their extractions collected via centrifugation, and medium containing zinc chloride (ZnCl₂), which released the same concentration of zinc as ZnO-NP suspensions in the culture medium. The A549 cell line was used in this study since nanoparticles have been reported to be capable of reaching the alveoli and causing pulmonary inflammation [23, 24]. The A549 cell line is derived from a human lung adenocarcinoma and has been used extensively in airborne particle toxicity studies [12, 25-27] because it maintains most of the characteristics of type II alveolar epithelial cells [28], which play important roles in responding to lung damage and contribute to various pulmonary immunology and inflammatory activities [29].

Materials and methods

1. Preparation and characterization of the exposure media

ZnO-NPs were purchased from Sigma-Aldrich (MO, USA), and ZnCl₂ was purchased from WAKO, Ltd., Osaka, Japan. We prepared 3 types of exposure media with these reagents. The first was the suspension: ZnO-NPs were dispersed into sterilized MiliQ water with sonication for 30 min, diluted with Dulbecco's Modified Eagle Medium containing 10% fetal bovine serum (hereafter referred to as supplemented DMEM or medium) to 25, 50, 75, or 100 µg / mL. The hydrodynamic diameter distribution of the ZnO-NP suspension was measured with a laser diffraction particle size analyzer (DLS6000AL, Otsuka Electronics Co., Ltd., Osaka, Japan). The second exposure medium was the extraction: the ZnO-NPs suspensions were incubated in a 37°C, 5% CO₂ incubator for 24 h, and the solid particles were then removed by centrifugation at 150,000 × g for 1 h at 4°C. The third exposure medium was ZnCl₂ medium: ZnCl₂ was dissolved in sterilized MiliQ water and then diluted with medium to the desired concentration. The concentration of the released zinc in the extractions and the ZnCl₂ medium was determined with a zinc colorimetric assay kit (AKJ Global Technology Co., Ltd., Chiba, Japan).

2. Cell culture and cytotoxicity assays

A549 cells were seeded in culture dishes with a density of 8,000 cells/cm² and incubated for 48 h at 37°C with 5% CO₂. The culture medium was then replaced with 1 of the 3 types of exposure media. After 24 h of exposure, cytotoxicity was assayed through morphological observation with a Cell Double Staining Kit (Dojindo, Kumamoto, Japan), WST cell viability assays using a Cell Counting Kit-8 (CCK-8, Dojindo), and LDH leakage assays using a CytoTox96 Non-radioactive Cytotoxicity Assay Kit (Promega Corporation, Madison, WI, USA). The assays were conducted according to the corresponding kits' protocols.

3. Global gene expression analysis

Total RNA of cells surviving the exposure was extracted with ISOGEN (Nippon Gene Co. Ltd.,

Tokyo, Japan) and purified from the protein and DNA contents with Recombinant DNaseI (Takara Bio, Inc., Shiga, Japan). An Amino Allyl MessageAmp II Arna Amplification Kit (Ambion, TX, USA) was used for the subsequent sample preparation for microarray analysis. We published the sample preparation and scanning procedure previously [30]. Finally, locally weighted scatter plot smoothing (LOWESS) adjustment was applied, and the expression of global genes was transited into corresponding numerical values. Function analysis was conducted via PANTHER's Gene Ontology (GO) biological process categories database (www.pantherdb.org/tools/genexAnalysis.jsp), and the regulated genes were classified into 3 broad functional categories, including "biological process," "cellular function," and "molecular function." Each broad category had a hierarchical structure, and the corresponding genes could be further classified in more detailed functional categories. The function annotation of each gene was calculated with Fisher's exact test to determine the *p*-value, which represented the statistical significance of the concordance rate between each category and the functional annotation of each gene [31]. Unless the *p*-value was less than 10^{-4} ($p < 0.0001$), the regulated genes were not considered as an inevitable response to the stress.

4. Inhibiting the expression of the metallothionein gene with siRNA

Lipofectamine™ RNAiMAX (Invitrogen, Carlsbad, CA, USA) was used as a transfection reagent. The transfection mixture was prepared, kept at room temperature for 20 min, and was then added to the cells with the exposure medium. After 24 h of incubation, the cells were collected and used for subsequent cytotoxicity assays or reverse transcription polymerase chain reaction (RT-PCR). For RT-PCR, total RNA was collected with ISOGENE (Nippon Gene Co. Ltd.), purified with Recombinant DNaseI (Takara Bio, Inc.), reverse transcribed into cDNA using a PrimerScript RT reagent kit (Takara Bio, Inc.), and finally stained with LightCycler Fast Start DNA Master SYBR Green I (Roche Applied Science Corp., Germany). The fluorescence intensity was

scanned with a LightCycler instrument (CAROUSEL, Roche Applied Science Corp.) and analyzed with corresponding software.

5. Detecting intracellular ROS

The OxiSelect™ Intracellular ROS Assay Kit (Green Fluorescence) was purchased from Cell Biolab, Inc. (CA, USA). The assay kit employed the cell-permeable fluorogenic probe 2', 7'-dichlorodihydrofluorescein diacetate (DCFH-DA), a well-established reagent for detecting intracellular ROS [32-34]. The exposed cells in opaque 96-well plates were washed twice with DPBS and then incubated in medium containing 100 μ M of DCFH-DA at 37°C and 5% CO₂ for 60 min. The fluorescence intensity was then determined with a microplate reader at an excitation of 485 nm and an emission of 530 nm. N-acetyl-L-cysteine (NAC, Sigma-Aldrich), a precursor of intracellular cysteine that can transform into glutathione in cells in order to enhance the intracellular reduction state by increasing the reduced/oxidized glutathione (GSH / GSSG) rate [35], was used to confirm the contribution of ROS to cytotoxicity. A549 cells were pretreated with 10 mM NAC for 2 h, and the medium was then replaced with exposure medium. After another 24-h exposure, cell viability was assayed with the CCK-8 kit.

6. Experimental design and statistical analysis

Unexposed cells were used as a negative control. Each experiment was conducted with 3 parallel samples and repeated independently 3 times. The results were analyzed with 2-tailed Student's *t*-tests. The results were considered significantly different from the control group if $p < 0.05$.

Results

1. Characterization of ZnO-NP suspensions in supplemented DMEM

We previously reported that the dimensions of ZnO-NPs were less than 60 nm, which is consistent with the nominal dimensions of the particles as determined by the supplier [36]. When the concentrations of the ZnO-NP suspensions ranged from 25 to 100 μ g / mL, the mean hydrodynamic diameters of freshly prepared suspensions ranged from 394.7 to 529.3 nm and the

mean hydrodynamic diameters ranged from 352.2 to 591.8 nm after incubation or 24 h (Table 1). The concentration of the released zinc in the suspensions was determined using the corresponding extractions and ranged from 6.09 to 9.18 $\mu\text{g} / \text{mL}$; when the particle concentration was more than 75 $\mu\text{g} / \text{mL}$, the released zinc reached the saturation concentration, about 9.18 $\mu\text{g} / \text{mL}$ (Table 2).

2. Cytotoxicity of ZnO-NP suspensions, their extractions, and ZnCl₂ medium

After A549 cells were exposed to 50, 75, or 100 $\mu\text{g} / \text{mL}$ ZnO-NP suspensions for 24 h, cell viability decreased by approximately 20%, 30%, and 60%, respectively, while no change was evident in the case of exposure to 25 $\mu\text{g} / \text{mL}$ ZnO-NP suspension (Figure 1a, b). In addition, the LDH leakage assay revealed that exposure to

Table 1 Mean hydrodynamic diameter of ZnO-NPs in supplemented DMEM.

Concentration of ZnO-NPs ($\mu\text{g}/\text{mL}$)	Mean diameter (nm)	
	Freshly prepared medium	24 h-incubated medium
25	525.3	591.8
50	529.3	431.4
75	394.7	449.5
100	406.1	352.2

Abbreviations: DMEM: Dulbecco's Modified Eagle Medium; ZnO-NPs: zinc oxide nanoparticles.

Table 2 Concentration of released zinc in ZnO-NP suspensions.

ZnO-NPs ($\mu\text{g} / \text{mL}$)	Released zinc ($\mu\text{g} / \text{mL}$)
25	6.09
50	7.85
75	9.18
100	9.18

Abbreviation: ZnO-NPs: zinc oxide nanoparticles.

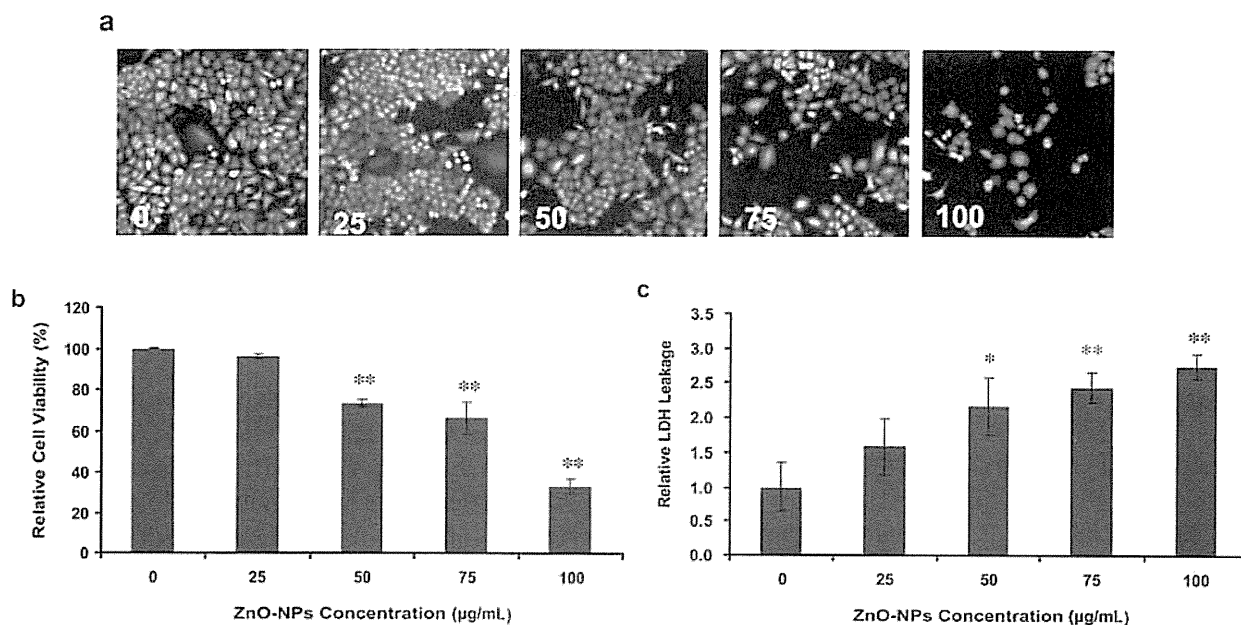


Figure 1 Cytotoxicity induced by ZnO-NP suspensions. A549 cells were exposed to 25, 50, 75, or 100 $\mu\text{g}/\text{mL}$ of ZnO-NP suspensions for 24 h, and cell viability was assayed with (a) cell staining, (b) WST, or (c) LDH leakage assay. ** $p < 0.01$, * $p < 0.05$.

Table 3 The number of genes regulated by different treatments.

	ZnO-NP medium 100 µg / mL	ZnCl ₂ medium 20 µg / mL
Upregulated genes	206	29
Downregulated genes	113	37

Abbreviation: ZnO-NPs: zinc oxide nanoparticles.

Table 4 Cadmium ion binding functional category genes regulated by different treatments.

Gene name	Fold change	
	100 µg / mL ZnO-NPs	20 µg / mL ZnCl ₂
MT1F	5.02	3.53
MT1A	4.90	1.45
MT1B	3.74	1.09
MT1E	3.73	<1.00
MT1L	2.73	<1.00

Abbreviation: ZnO-NPs: zinc oxide nanoparticles.

50, 75, and 100 µg / mL ZnO-NP suspensions also resulted in loss of the integrity of the plasma membrane (Figure 1c). In contrast, zinc released from ZnO-NPs did not cause a reduction in cell viability or have adverse effects on cell number and the integrity of the plasma membrane (Figure 2a-c).

3. Global gene expression analysis

To identify which gene functional categories were regulated in response to ZnO-NPs and released zinc, we conducted cDNA microarray analysis of cells exposed to 100 µg / mL ZnO-NP suspension or 20 µg / mL ZnCl₂. We used 20 µg / mL ZnCl₂ as the released zinc control in the absence of the solid particles to avoid possible interference from released impurities in the extractions and because we found that medium treated with 20 µg / mL ZnCl₂ contained about 10 µg/mL released zinc (data not shown), which was equivalent to that of the 100 µg / mL ZnO-NP suspension. In response to the 100 µg / mL ZnO-NP suspension, 206 and 113 genes were up- or downregulated, respectively; in contrast, in response to 20 µg / mL ZnCl₂ medium, 29 and 37 genes were up- or downregulated, respectively (Table 3 and Table S1–S4). Through the subsequent data mining on the regulated genes via PANTHER’s GO biological process categories database, the same functional gene category, “cadmium ion binding,” was identified in response to both the ZnO-NP suspension and the ZnCl₂ treatment. The “cadmium ion binding” category consisted of 5 MT isomer genes: MT1F, MT1A, MT1B, MT1E, and MT1L. The fold change of MT expression is summarized in Table 4. No significantly changed functional category was identified among the downregulated genes.

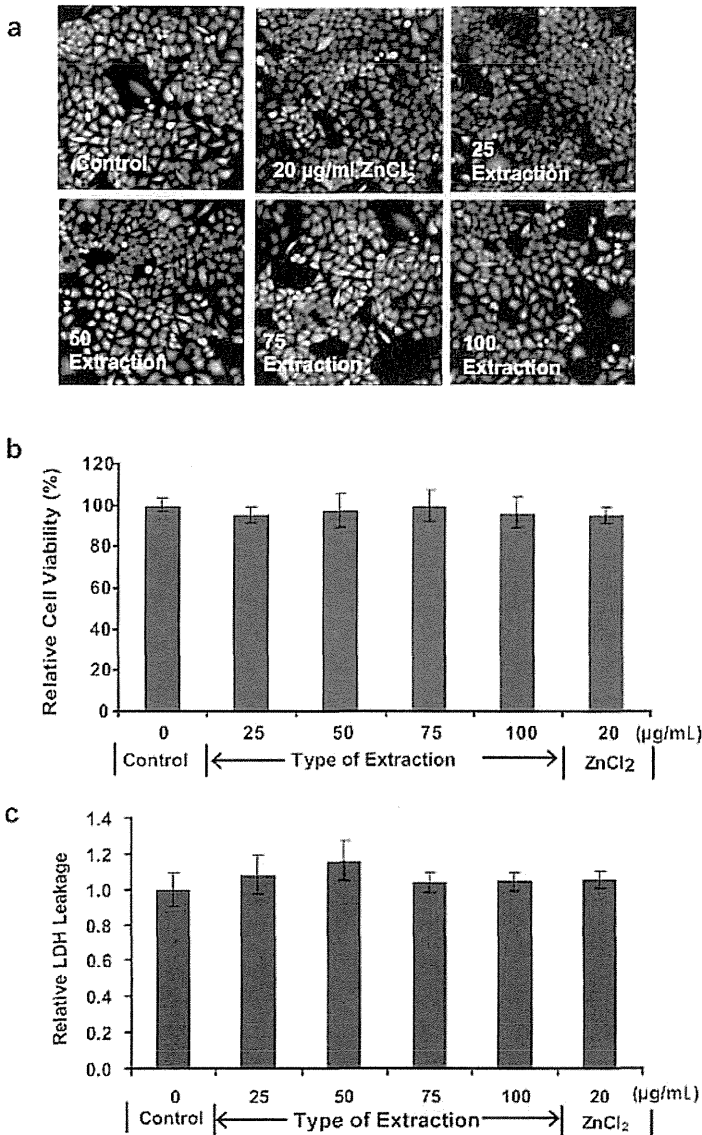


Figure 2 Cytotoxicity induced by 20 µg/mL ZnCl₂ or ZnO-NP extraction. A549 cells were exposed to 20 µg/mL ZnCl₂ and extractions of the 25, 50, 75, and 100 µg/mL ZnO-NP suspensions for 24 h, and cell viability was assayed with a) cell staining, b) WST, and c) LDH leakage assay. ** $p < 0.01$, * $p < 0.05$.

4. Cytotoxicity in the absence of MT overexpression

To confirm the role of MT in ZnO-NP-induced cytotoxicity, we inhibited MT expression with corresponding siRNA during 24-h exposure to ZnO-NPs or ZnCl₂. In the case of exposure to ZnO-NPs, the siRNA transfection inhibited MT expression to 1.4% of the corresponding control, while in the case of the ZnCl₂ exposure, the

siRNA transfection inhibited the MT expression to 1.1% of the corresponding control (Table 5). We then assayed cell viability. Inhibiting MT expression resulted in a decrease in cell viability to about 88%, 80%, and 53% of the control in 50, 75, and 100 µg / mL ZnO-NP suspensions, respectively, but had no effect on the viability of cells exposed to the extractions or the ZnCl₂ medium (Figure 3).

Table 5 MT1F inhibition efficiency of MT isomer gene expression.

	100 µg / mL ZnO-NPs	20 µg / mL ZnCl ₂
Control ^a	1	1
MTs siRNA	0.014	0.011

^aThe expression of MTs in cells transfected with a random RNA sequence was used as a control, and the expression of MT in cells transfected with MT siRNA was calculated to be a portion of the control. Abbreviations: ZnO-NPs: zinc oxide nanoparticles; MT: metallothionein.

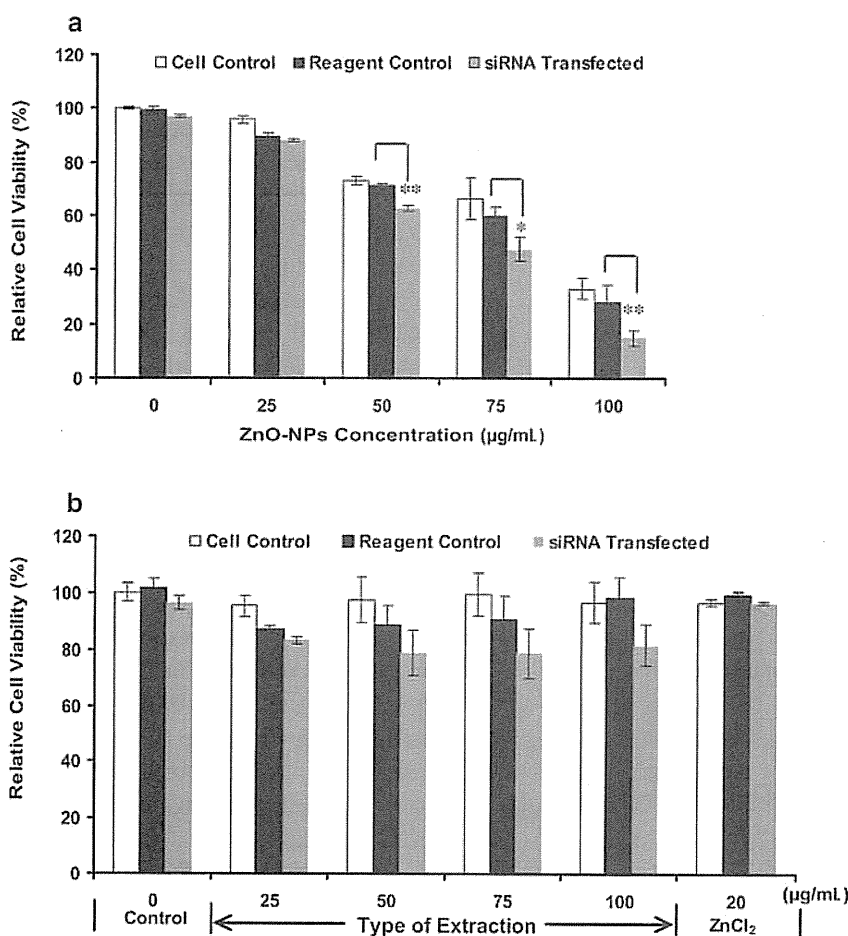


Figure 3 Function of MTs in response to the various exposures. MT expression in A549 cells was inhibited with corresponding siRNA during exposure to (a) suspensions of 25, 50, 75, or 100 µg/mL ZnO-NPs or (b) their extractions or 20 µg/mL ZnCl₂ for 24 h. Cell viability was assayed with WST. The statistical significance was analyzed by comparing siRNA-transfected cells with corresponding reagent controls. ** $p < 0.01$, * $p < 0.05$.

5. Intracellular ROS

Intracellular ROS was detected when ZnO-NPs were more than 50 $\mu\text{g}/\text{mL}$; however, no ROS generation was observed in the cells exposed to ZnCl_2 (Figure 4). To examine whether ROS induced by ZnO-NPs was involved in cytotoxicity, cells were pretreated with NAC before exposure to ZnO-NPs. As shown in Figure 5, cell viability was partially recovered by NAC treatment in cells treated with 50 $\mu\text{g}/\text{mL}$ and 75 $\mu\text{g}/\text{mL}$ ZnO-NPs. However, in the case of the 100 $\mu\text{g}/\text{mL}$ ZnO-NP suspension, NAC pretreatment had no effect on the cell viability.

6. Synergic toxicity of ROS and zinc

Next, we incubated A549 cells in the exposure medium containing ZnCl_2 and / or H_2O_2 for 24 h. According to the concentration of H_2O_2 , exposure media were designed as 0 mM, 0.5 mM, and 1 mM; in each group, the concentration of ZnCl_2 ranged from 0 to 50 $\mu\text{g}/\text{mL}$. Cell viability was assayed after a 24-h incubation. As shown in Figure 6, in absence of H_2O_2 , 20 $\mu\text{g}/\text{mL}$ ZnCl_2 had no effect on cell viability; however, in presence of 0.5 or 1 mM H_2O_2 , 20 $\mu\text{g}/\text{mL}$ ZnCl_2 reduced cell viabilities to about 83% and 50% of the control, respectively. In the case

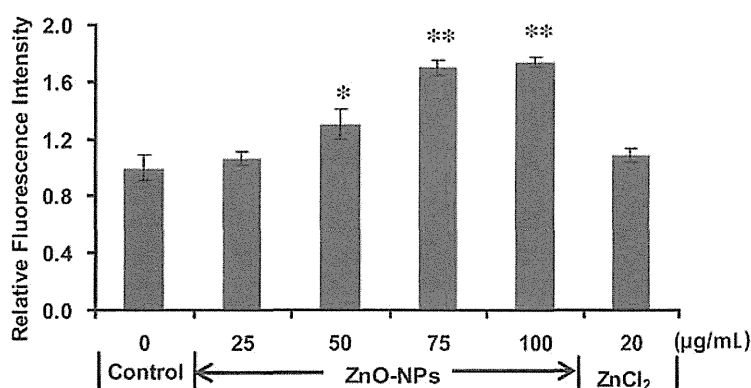


Figure 4 The intracellular ROS assay with DCFH-DA. The fluorescence intensity is directly proportional to the intracellular ROS concentration. ** $p < 0.01$, * $p < 0.05$.

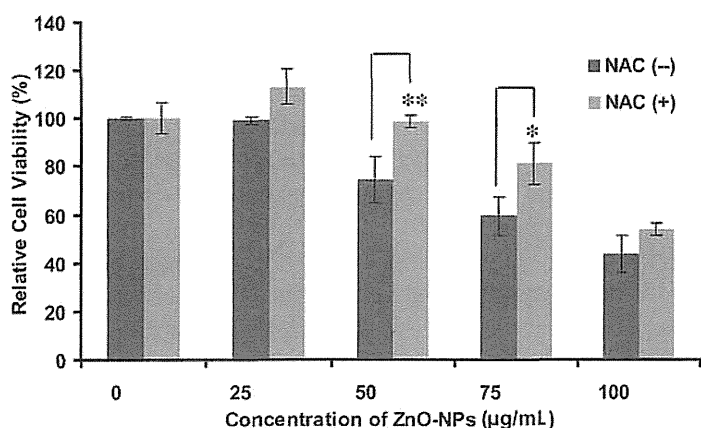


Figure 5 Changes in cell viability after NAC pre-incubation. After pre-incubated with NAC for 2 h, A549 cells were exposed to ZnO-NPs for another 24 h, and cell viability was assayed with WST. ** $p < 0.01$, * $p < 0.05$.

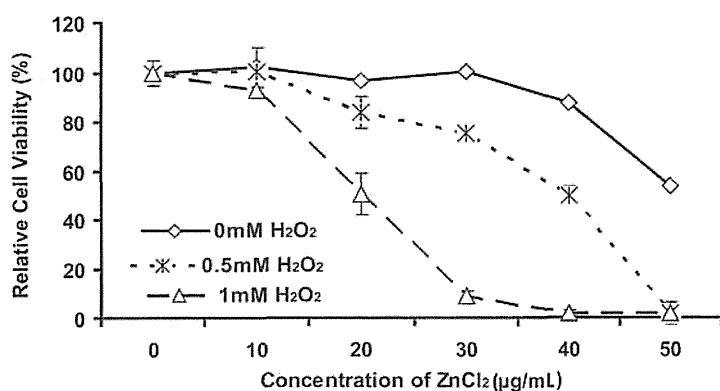


Figure 6 The synergic effect of H_2O_2 and zinc. The results are presented as the percentage of the control (0 mM ZnCl_2) of the corresponding group. The statistical significance of the change in cell viability was analyzed by comparing with the control series.

of 30 $\mu\text{g} / \text{mL}$ ZnCl_2 , there was no change in cell viability in absence of H_2O_2 , while in presence of 0.5 or 1 mM of H_2O_2 , cell viability decreased to 75% and 10%, respectively. Treatment with 40 $\mu\text{g} / \text{mL}$ ZnCl_2 resulted in a decrease in relative cell viability to 0 in presence of 1 mM H_2O_2 , but decreased cell viability by only about 15% in the absence of H_2O_2 and by about 40% in the presence of 0.5 mM H_2O_2 .

Discussion

1. The exposure design

The dissolution of zinc oxide is a well-described phenomenon that occurs over a wide range of pH values [37]. In water at pH 7.5, the overall dissolution reaction of zinc oxide can be shortly written as follows: $\text{ZnO} (\text{s}) \rightleftharpoons \text{Zn}^{2+} (\text{aq}) + \text{OH} (\text{aq})$ [38, 39]. Franklin *et al.* discussed the importance of the water solubility of ZnO-NPs in their toxicity study on microalga [20]. However, in previous studies, the solubility and saturation of ZnO-NPs in different culture media were rarely taken into consideration, which resulted in ZnO-NP cytotoxicity being compared with the toxicity of zinc salt consisting of the equivalent moles of zinc rather than zinc salt with the same capability to release zinc in the solvent [18, 22, 40]. This introduces the risk of not accurately estimating true exposure and the possibility of over- or underestimating the effects of the released zinc. Since the objective of this study was to identify the respective contributions of released zinc and solid particles on the cytotoxicity of ZnO-NPs, we used ZnO-NP extractions to control for the zinc released from the ZnO-NP suspension in the cytotoxicity assay.

For the global gene expression analysis, we used ZnCl_2 medium as the released zinc control to avoid potential interference from impurities in the extractions. We measured the concentration of released zinc in the ZnO-NP suspensions and ZnCl_2 medium using a zinc-specific chelator [41] and found that the released zinc in 100 $\mu\text{g}/\text{mL}$ of the ZnO-NP suspension reached the saturation concentration, about 9.18 $\mu\text{g} / \text{mL}$, which was equivalent to the zinc concentration in 20 $\mu\text{g} / \text{mL}$ of ZnCl_2 medium. Therefore, we used the 20 $\mu\text{g} / \text{mL}$ ZnCl_2 medium concentration as a control for the released zinc from the 100 $\mu\text{g} / \text{mL}$ ZnO-NP suspension in our gene

expression analysis. Additionally, using the saturation zinc concentration of the ZnO-NPs, we could avoid the potential interference of the “bound zinc/free zinc” ratio induced by different solubilities since this issue has not been studied clearly [42-44]. Bound zinc and free zinc are different forms of released zinc in supplemented DMEM. The zinc binding capacity of DMEM has garnered concerns in *in vitro* studies. Part of the total zinc is localized by zinc ligands in DMEM; therefore, the total released zinc can be separated into 2 groups: free zinc and bound zinc, which binds to protein components in the medium [45, 46]. Here, we attempted to address this problem by measuring the total released zinc using a zinc-specific chelator. However, we are continuing to work on this issue since the effects of free zinc and bound zinc on *in vitro* toxicity have not been fully elucidated [17].

2. Both solid particles and released zinc contribute to ZnO-NP-dependent cytotoxicity

With the above modification, we found that the ZnO-NP suspension reduced the cell viability, damaged the integrity of the plasma membrane, and induced abnormal cell morphologies; however, neither the extractions nor the ZnCl_2 medium showed adverse effects on A549 cells. These findings indicated the importance of solid particles for ZnO-NP-induced cytotoxicity and are consistent with the predictions of Moos *et al.*, who hypothesized that the presence of solid particles was necessary for ZnO-NP-induced cytotoxicity [14].

Our subsequent global gene expression analysis revealed that the same functional category, “cadmium ion binding,” was upregulated in response not only to ZnCl_2 , but also to ZnO-NPs, despite the fact that these 2 treatments exhibited the opposite effects on exposed cells (nontoxic and toxic, respectively). The “cadmium ion binding” category consisted of MTs that belong to the well-studied cysteine-rich metalloprotein family. MTs play important roles in maintaining the intracellular homeostasis of heavy metals via binding, exchanging, and transporting heavy metals, such as zinc, cadmium, and copper, with their cysteine residues [47, 48]. For example, when cells are suddenly exposed to high levels of zinc, apo-MTs capture

excessive intracellular zinc, reducing it to non-toxic levels, while the cells upregulate the expression of MTs via metal regulatory transcription factor 1 (MTF1)-mediated feedback [49]. Additionally, MTs are also reported to act as intracellular antioxidants to quench ROS in some special cases [50]. In the current study, we exposed A549 cells to medium containing H₂O₂ and found no change in the expression of MT. Accordingly, we could rule out the possibility that the overexpression of MTs occurred in response to ROS and thus proposed that A549 cells upregulated MTs in response to ZnCl₂ and released zinc generated by ZnO-NPs, which have been reported to produce ROS [12, 16, 17, 22]. To identify the role of the released zinc in our exposures, we inhibited the expression of MT using corresponding siRNA and found that the toxicity of the 100 µg / mL ZnO-NP suspension was enhanced when MT expression was inhibited. This result indicated that the released zinc contributed to ZnO-NP-induced cytotoxicity. The cytotoxicity of the excessive zinc has been reported to inhibit cellular respiration [51, 52] and the key enzymes in the glycolytic pathway, leading to ATP depletion in cells [53, 54].

3. The synergic relationship between solid particles and released zinc in ZnO-NP-induced cytotoxicity

Interestingly, inhibiting the expression of MT did not affect the viability of the cells exposed to the extractions or 20 µg/mL ZnCl₂, indicating that the released zinc did not have a substantial effect on the cells in the absence of solid particles.

The “Trojan-horse” theory has been likened to the role of solid particles in ZnO-NPs: nanoparticles bring zinc ions into cells through particle internalization by cells, similar to how the Greeks were brought into the city of Troy by the wooden horse, leading to adverse effects and even cell death [21, 40]. Although one report has demonstrated the internalization of ZnO-NPs by A549 cells [12], no data has yet demonstrated the proportional correlation of uptake and cytotoxicity. In this study, we also observed exposed cells and rarely found endocytosis of the particles by A549 cells (data not shown). The other possibility is that the particles generate ROS,

since ROS is thought to be the most important mechanism of nanotoxicity [55]. With DCFH, we detected intracellular ROS following exposure to ZnO-NPs, but not following exposure to the ZnCl₂ medium. Furthermore, when we pre-treated A549 cells with NAC, a precursor of intracellular antioxidants, cell viability was recovered, unlike in untreated cells. Thus, we concluded that ROS contributed to ZnO-NP-induced cytotoxicity via solid particles.

In the case of the nanoparticles of transient metal oxides, such as copper oxide (CuO-NPs) and iron oxide, ROS is thought to be produced by the dissolved metal ions via Fenton’s reaction [21, 22]. However, divalent zinc is not redox reactive and is not usually thought to cause Fenton’s reaction [19, 56]. In a previous study, we also demonstrated the different toxic behaviors of a typical transient metal oxide, CuO-NPs, and a semiconductive material, ZnO-NPs [36]. The oxidation potential of ZnO nanomaterial has been attributed to its unique surface properties resulting from the quantum size of the particles [1, 57-59]. Thus, we propose the special surface reactivity of ZnO-NPs is the reason for the necessity of the solid particles in ZnO-NP-dependent cytotoxicity.

To demonstrate the relationship between ROS and released zinc in ZnO-NP-induced cytotoxicity, we exposed A549 cells to ZnCl₂ and H₂O₂ simultaneously. We found that the toxicity of released zinc was enhanced by H₂O₂, similar to a report by Heng *et al.* demonstrating that the cytotoxicity of ZnO-NPs was aggravated by exogenous ROS [15]. Zhang explained that ROS could incapacitate MTs via oxidation of sulfhydryl groups, leading to an increase in intracellular free zinc to toxic levels [60]. We propose that the solid particles produce ROS via their special surface activity, and the generated ROS can then incapacitate MT, the most important protein involved in maintaining intracellular zinc homeostasis, finally allowing intracellular free zinc to reach toxic levels.

The findings of this study indicated that both solid particles and released zinc contribute to the cytotoxicity of ZnO-NPs, while released zinc alone does not cause substantial toxicity in A549 cells in the absence of solid particles. Moreover, we propose that released zinc and

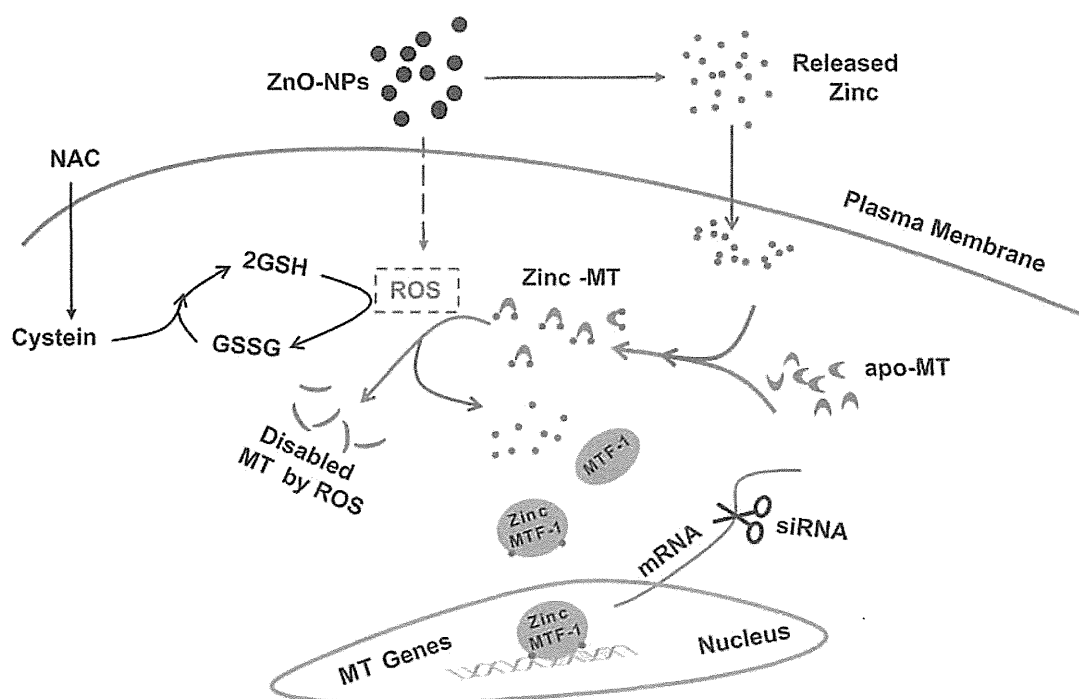


Figure 7 Synergistic toxicity of solid particles and released zinc from ZnO-NPs in A549 cells. Once dispersed into the cell culture medium, ZnO-NPs release zinc and generate ROS. To maintain the homeostasis of intracellular free zinc, A549 cells upregulate the expression of apo-MTs via the zinc-MTF1 complex. ROS not only destroy the intracellular redox status, they also oxidize the MTs, resulting in the zinc defense breakdown.

solid particles have a synergistic effect on toxicity as follows: in response to the excessive released zinc generated by ZnO-NPs, A549 cells upregulate the expression of MT; the solid particles produce ROS via their special surface chemical reactions and inhibit MT, thereby leading to the breakdown of the defense against the excessive intracellular free zinc (Figure 7).

Nowadays, human exposure to engineered nanoparticles is inevitable since nanoparticles are becoming more and more widely used. Our previous knowledge of airborne pollutant particles, such as diesel exhaust, provides important details on the toxicology of ultrafine particles (<100 nm), especially in established ROS models for toxicological mechanisms of particulate materials [61]. However, unlike the similarity with airborne pollutant particles, engineered nanomaterials have physicochemical properties distinct to their different chemical compositions. Thus, we must consider true exposure to nanomaterials on a case-by-case basis to determine cytotoxicity to each biological system, and this will become very important in evaluating the toxic potential of nanoparticles and improving

engineered nanomaterials. We also suggest that both the nanoscaled superficial properties and the dissolved chemical composition of nanosized metal oxides should be characterized fully. Moreover, the synergistic effects of these particles should be determined in future studies.

Acknowledgments

We would like to thank Ms. H. Morita and Dr. T. Takemura for technical assistance. This work was supported by a Grant-in-Aid from the Ministry of Health, Labour, and Welfare of Japan.

References

- 1) Fan Z, Lu J G. Zinc oxide nanostructures: synthesis and properties. *J Nanosci Nanotechnol* 2005; 5: 1561-1573.
- 2) Djurišić A B, Leung Y H. Optical properties of ZnO nanostructures. *Small* 2006; 2: 944-961.
- 3) Banerjee D, Lao J Y, Wang D Z, Huang J Y, Steeves D, Kimball B, Ren Z F. Synthesis and photoluminescence studies on ZnO nanowires. *Nanotechnology* 2004; 15: 404-409.
- 4) De Berardis B, Civitelli G, Condello M, Lista P, Pozzi R, Arancia G, Meschini S. Exposure to ZnO nanoparticles induces oxidative stress and cytotoxicity in human colon carcinoma cells.

- Toxicol Appl Pharmacol 2010.[Epub ahead of print]
- 5) Ostrowski A D, Martin T, Conti J, Hurt I, Harthorn B H. Nanotoxicology: characterizing the scientific literature, 2000-2007. *J Nanopart Res* 2009; 11: 251-257.
 - 6) OECD. Guidance Manual for the Testing of Manufactured Nanomaterials: OECD's Sponsorship Programme. 2009.
 - 7) Zhu X S, Zhu L, Duan Z H, Qi R Q, Li Y, Lang Y P. Comparative toxicity of several metal oxide nanoparticle aqueous suspensions to Zebrafish (*Danio rerio*) early developmental stage. *J Environ Sci Heal A* 2008; 43: 278-284.
 - 8) Wiench K, Wohlleben W, Hisgen V, Radke K, Salinas E, Zok S, Landsiedel R. Acute and chronic effects of nano- and non-nano-scale TiO₂ and ZnO particles on mobility and reproduction of the freshwater invertebrate *Daphnia magna*. *Chemosphere* 2009; 76: 1356-1365.
 - 9) Lin D H, Xing B S. Phytotoxicity of nanoparticles: Inhibition of seed germination and root growth. *Environ Pollut* 2007; 150: 243-250.
 - 10) Jones N, Ray B, Ranjit K T, Manna A C. Antibacterial activity of ZnO nanoparticle suspensions on a broad spectrum of microorganisms. *FEMS Microbiol Lett* 2008; 279: 71-76.
 - 11) Jeng H A, Swanson J. Toxicity of metal oxide nanoparticles in mammalian cells. *J Environ Sci Heal A* 2006; 41: 2699-2711.
 - 12) Lin W S, Xu Y, Huang C C, Ma Y F, Shannon K B, Chen D R, Huang Y W. Toxicity of nano- and micro-sized ZnO particles in human lung epithelial cells. *J Nanoparticle Res* 2009; 11: 25-39.
 - 13) Gojova A, Guo B, Kota R S, Rutledge J C, Kennedy I M, Barakat A I. Induction of inflammation in vascular endothelial cells by metal oxide nanoparticles: effect of particle composition. *Environ Health Perspect* 2007; 115: 403-409.
 - 14) Moos P J, Chung K, Woessner D, Honegger M, Cutler N S, Veranth J M. ZnO Particulate Matter Requires Cell Contact for Toxicity in Human Colon Cancer Cells. *Chem Res Toxicol* 2010; 23: 733-739.
 - 15) Heng B C, Zhao X X, Xiong S J, Ng K W, Boey F Y C, Loo J S C. Toxicity of zinc oxide (ZnO) nanoparticles on human bronchial epithelial cells (BEAS-2B) is accentuated by oxidative stress. *Food Chem Toxicol* 2010; 48: 1762-1766.
 - 16) Sharma V, Shukla R K, Saxena N, Parmar D, Das M, Dhawan A. DNA damaging potential of zinc oxide nanoparticles in human epidermal cells. *Toxicol Lett* 2009; 185: 211-218.
 - 17) Yin H, Casey P S, McCall M J, Fenech M. Effects of surface chemistry on cytotoxicity, genotoxicity, and the generation of reactive oxygen species induced by ZnO nanoparticles. *Langmuir* 2010; 26: 15399-15408.
 - 18) Brunner T J, Wick P, Manser P, Spohn P, Grass R N, Limbach L K, Bruinink A, Stark W J. In vitro cytotoxicity of oxide nanoparticles: comparison to asbestos, silica, and the effect of particle solubility. *Environ Sci Technol* 2006; 40: 4374-4381.
 - 19) Eigen M. Fast elementary steps in chemical reaction mechanisms. *Pure Appl Chem* 1963; 6: 97-116.
 - 20) Franklin N M, Rogers N J, Apte S C, Batley G E, Gadd G E, Casey P S. Comparative toxicity of nanoparticulate ZnO, bulk ZnO, and ZnCl₂ to a freshwater microalga (*Pseudokirchneriella subcapitata*): the importance of particle solubility. *Environ Sci Technol* 2007; 41: 8484-8490.
 - 21) Limbach L K, Wick P, Manser P, Grass R N, Bruinink A, Stark W J. Exposure of engineered nanoparticles to human lung epithelial cells: Influence of chemical composition and catalytic activity on oxidative stress. *Environ Sci Technol* 2007; 41: 4158-4163.
 - 22) Xia T, Kovochich M, Liang M, Madler L, Gilbert B, Shi H B, Yeh J I, Zink J I, Nel A E. Comparison of the mechanism of toxicity of zinc oxide and cerium oxide nanoparticles based on dissolution and oxidative stress properties. *ACS Nano* 2008; 2: 2121-2134.
 - 23) Heyder J. Deposition of inhaled particles in the human respiratory tract and consequences for regional targeting in respiratory drug delivery. *Proc Am Thorac Soc* 2004; 1: 315-320.
 - 24) Muhlfeld C, Rothen-Rutishauser B, Blank F, Vanhecke D, Ochs M, Gehr P. Interactions of nanoparticles with pulmonary structures and cellular responses. *Am J Physiol Lung Cell Mol Physiol* 2008; 294: L817-829.
 - 25) Singh S, Shi T, Duffin R, Albrecht C, Van Berlo D, Hohl D, Fubini B, Martra G, Fenoglio I, Borm P J, Schins R P. Endocytosis, oxidative stress and IL-8 expression in human lung epithelial cells upon treatment with fine and ultrafine TiO₂: role of the specific surface area and of surface methylation of the particles. *Toxicol Appl Pharmacol* 2007; 222: 141-151.
 - 26) Kim J S, Yoon T J, Yu K N, Noh M S, Woo M, Kim B G, Lee K H, Sohn B H, Park S B, Lee J K, Cho M H. Cellular uptake of magnetic nanoparticle is mediated through energy-dependent endocytosis in A549 cells. *J Vet Sci* 2006; 7: 321-326.
 - 27) Stringer B, Kobzik L. Environmental particulate-mediated cytokine production in lung epithelial cells (A549): role of preexisting inflammation and oxidant stress. *J Toxicol Environ Health A* 1998; 55: 31-44.
 - 28) Foster K A, Oster C G, Mayer M M, Avery M L, Audus K L. Characterization of the A549 cell line as a type II pulmonary epithelial cell

- model for drug metabolism. *Exp Cell Res* 1998; 243: 359-366.
- 29) Thompson A B, Robbins R A, Romberger D J, Sisson J H, Spurzem J R, Teschler H, Rennard S I. Immunological functions of the pulmonary epithelium. *Eur Respir J* 1995; 8: 127-149.
 - 30) Hanagata N, Zhuang F, Connolly S, Li J, Ogawa N, Xu M S. Molecular responses of human lung epithelial cells to the toxicity of copper oxide nanoparticles inferred from whole genome expression analysis. *ACS Nano* 2011; 5: 9326-9338.
 - 31) Hosack D A, Dennis G, Sherman B T, Lane H C, Lempicki R A. Identifying biological themes within lists of genes with EASE. *Genome Biol* 2003; 4.
 - 32) Keller A, Mohamed A, Drose S, Brandt U, Fleming I, Brandes R P. Analysis of dichlorodihydrofluorescein and dihydrocalcein as probes for the detection of intracellular reactive oxygen species. *Free Radical Res* 2004; 38: 1257-1267.
 - 33) Halliwell B, Whiteman M. Measuring reactive species and oxidative damage in vivo and in cell culture: how should you do it and what do the results mean? *Brit J Pharmacol* 2004; 142: 231-255.
 - 34) Wang H, Joseph J A. Quantifying cellular oxidative stress by dichlorofluorescein assay using microplate reader. *Free Radic Biol Med* 1999; 27: 612-616.
 - 35) Kowaltowski A J, Vercesi a E. Mitochondrial damage induced by conditions of oxidative stress. *Free Radic Biol Med* 1999; 26: 463-471.
 - 36) Xu M S, Fujita D, Kajiwara S, Minowa T, Li X L, Takemura T, Iwai H, Hanagata N. Contribution of physicochemical characteristics of nano-oxides to cytotoxicity. *Biomaterials* 2010; 31: 8022-8031.
 - 37) Bian S W, Mudunkotuwa I A, Rupasinghe T, Grassian V H. Aggregation and dissolution of 4 nm ZnO nanoparticles in aqueous environments: influence of pH, ionic strength, size, and adsorption of humic acid. *Langmuir* 2011; 27: 6059-6068.
 - 38) Degen A, Kosec M. Effect of pH and impurities on the surface charge of zinc oxide in aqueous solution. *J Eur Ceramic Soc* 2000; 20: 667-673.
 - 39) Yamabi S, Imai H. Growth conditions for wurtzite zinc oxide films in aqueous solutions. *J Mater Chem* 2002; 12: 3773-3778.
 - 40) Deng X Y, Luan Q X, Chen W T, Wang Y L, Wu M H, Zhang H J, Jiao Z. Nanosized zinc oxide particles induce neural stem cell apoptosis. *Nanotechnol* 2009; 20.
 - 41) Makino T, Saito M, Horiguchi D, Kina K. A highly sensitive colorimetric determination of serum zinc using water-soluble pyridylazo dye. *Clin Chim Acta* 1982; 120: 127-135.
 - 42) Bai W, Zhang Z Y, Tian W J, He X, Ma Y H, Zhao Y L, Chai Z F. Toxicity of zinc oxide nanoparticles to zebrafish embryo: a physicochemical study of toxicity mechanism. *J Nanoparticle Res* 2010; 12: 1645-1654.
 - 43) Nel A E, Madler L, Velegol D, Xia T, Hoek E M V, Somasundaran P, Klaessig F, Castranova V, Thompson M. Understanding biophysicochemical interactions at the nano-bio interface. *Nat Mater* 2009; 8: 543-557.
 - 44) Cedervall T, Lynch I, Lindman S, Berggard T, Thulin E, Nilsson H, Dawson K A, Linse S. Understanding the nanoparticle-protein corona using methods to quantify exchange rates and affinities of proteins for nanoparticles. *Proc Nat Acad Sci U S A* 2007; 104: 2050-2055.
 - 45) Bozym R A, Chimienti F, Giblin L J, Gross G W, Korichneva I, Li Y A, Libert S, Maret W, Parviz M, Frederickson C J, Thompson R B. Free zinc ions outside a narrow concentration range are toxic to a variety of cells in vitro. *Exp Biol Med* 2010; 235: 741-750.
 - 46) Lu J, Stewart a J, Sadler P J, Pinheiro T J T, Blindauer C A. Albumin as a zinc carrier: properties of its high-affinity zinc-binding site. *Biochem Soc Trans* 2008; 36: 1317-1321.
 - 47) Guan Y S. Comments to metallothionein as an anti-inflammatory mediator. *Mediat Inflamm* 2009.
 - 48) Inoue K I, Takano H, Shimada A, Satoh M. Metallothionein as an anti-inflammatory mediator. *Mediat Inflamm* 2009.
 - 49) Gyulhandanyan A V, Lee S C, Bikopoulos G, Dai F H, Wheeler M B. The Zn²⁺-transporting pathways in pancreatic beta-cells - a role for the L-type voltage-gated Ca²⁺ channel. *J Biol Chem* 2006; 281: 9361-9372.
 - 50) Vliagoftis A, Schwingshackl A, Milne C D, Duszyk M, Hollenberg M D, Wallace J L, Befus A D, Moqbel R. Proteinase-activated receptor-2-mediated matrix metalloproteinase-9 release from airway epithelial cells. *J Allergy Clin Immun* 2000; 106: 537-545.
 - 51) Sensi S L, Yin H Z, Carriedo S G, Rao S S, Weiss J H. Preferential Zn²⁺ influx through Ca²⁺-permeable AMPA/kainate channels triggers prolonged mitochondrial superoxide production. *Proc Nat Acad Sci U S A* 1999; 96: 2414-2419.
 - 52) Frazzini V, Rockabrand E, Mocchegiani E, Sensi S L. Oxidative stress and brain aging: is zinc the link? *Biogerontology* 2006; 7: 307-314.
 - 53) Dineley K E, Votyakova T V, Reynolds I J. Zinc inhibition of cellular energy production: implications for mitochondria and neurodegeneration. *J Neurochem* 2003; 85: 563-570.
 - 54) Gazaryan I G, Krasinskaya I P, Kristal B S, Brown A M. Zinc irreversibly damages major enzymes of energy production and antioxidant defense prior to mitochondrial permeability

- transition. *J Biol Chem* 2007; 282: 24373-24380.
- 55) Nel A, Xia T, Madler L, Li N. Toxic potential of materials at the nanolevel. *Science* 2006; 311: 622-627.
- 56) Nakamura M, Shishido N, Nunomura A, Smith M A, Perry G, Hayashi Y, Nakayama K, Hayashi T. Three histidine residues of amyloid-beta peptide control the redox activity of copper and iron. *Biochemistry* 2007; 46: 12737-12743.
- 57) Wang X D, Ding Y, Summers C J, Wang Z L. Large-scale synthesis of six-nanometer-wide ZnO nanobelts. *J Phys Chem B* 2004; 108: 8773-8777.
- 58) Kukreja L M, Barik S, Misra P. Variable band gap ZnO nanostructures grown by pulsed laser deposition. *J Cryst Growth* 2004; 268: 531-535.
- 59) Chiou J W, Kumar K P K, Jan J C, Tsai H M, Bao C W, Pong W F, Chien F Z, Tsai M H, Hong I H, Klauser R, Lee J F, Wu J J, Liu S C. Diameter dependence of the electronic structure of ZnO nanorods determined by x-ray absorption spectroscopy and scanning photoelectron microscopy. *Appl Phys Lett* 2004; 85: 3220-3222.
- 60) Zhang B, Georgiev O, Haggmann M, Gunes C, Cramer M, Faller P, Vasak M, Schaffner W. Activity of metal-responsive transcription factor 1 by toxic heavy metals and H₂O₂ in vitro is modulated by metallothionein. *Mol Cell Biol* 2003; 23: 8471-8485.
- 61) Li N, Sioutas C, Cho A, Schmitz D, Misra C, Sempf J, Wang M, Oberley T, Froines J, Nel A. Ultrafine particulate pollutants induce oxidative stress and mitochondrial damage. *Environ Health Perspect* 2003; 111: 455-460.

(Received: November 15, 2012/

Accepted: December 20, 2012)

Corresponding author:

Nobutaka HANAGATA, Ph.D.
Nanotechnology Innovation Station,
National Institute for Materials Science (NIMS)
1-2-1 Sengen, Tsukuba, Ibaraki 305-0047, Japan
Tel: +81-29-860-4774 Fax: +81-29-859-2475
E-mail: HANAGATA.Nobutaka@nims.go.jp

Table S1 List of the Genes Up-regulated by 100 µg / mL of ZnO-NPs in A549 cells.

Gene symbol	Description	Fold-change
MT1F	Homo sapiens metallothionein 1F (MT1F), mRNA [NM_005949]	5.02
MT1A	Homo sapiens metallothionein 1A (MT1A), mRNA [NM_005946]	4.90
MT1G	Homo sapiens metallothionein 1G (MT1G), mRNA [NM_005950]	4.31
LOC387763	Protein Ag2 homolog [Source:UniProtKB/Swiss-Prot;Acc:Q7Z7L8] [ENST00000339446]	4.29
MT2A	Homo sapiens metallothionein 2A (MT2A), mRNA [NM_005953]	3.93
IL1F7	Homo sapiens interleukin 1 family, member 7 (zeta) (IL1F7), transcript variant 1, mRNA [NM_014439]	3.90
MT1B	Homo sapiens metallothionein 1B (MT1B), mRNA [NM_005947]	3.74
MT1E	Homo sapiens metallothionein 1E (MT1E), mRNA [NM_175617]	3.73
EGR1	Homo sapiens early growth response 1 (EGR1), mRNA [NM_001964]	3.72
MT1X	Homo sapiens metallothionein 1X (MT1X), mRNA [NM_005952]	3.60
PTPRR	Homo sapiens protein tyrosine phosphatase, receptor type, R (PTPRR), transcript variant 1, mRNA [NM_002849]	3.51
SUSD5	Homo sapiens sushi domain containing 5 (SUSD5), mRNA [NM_015551]	3.40
SLC30A2	Homo sapiens solute carrier family 30 (zinc transporter), member 2 (SLC30A2), transcript variant 1, mRNA [NM_001004434]	3.30
MT1H	Homo sapiens metallothionein 1H (MT1H), mRNA [NM_005951]	3.11
HSPA6	Homo sapiens heat shock 70kDa protein 6 (HSP70B) (HSPA6), mRNA [NM_002155]	3.02
MT1L	Homo sapiens metallothionein 1L (gene/pseudogene) (MT1L), non-coding RNA [NR_001447]	2.73
ATF3	Homo sapiens activating transcription factor 3 (ATF3), transcript variant 4, mRNA [NM_001040619]	2.41
BEX2	Homo sapiens brain expressed X-linked 2 (BEX2), mRNA [NM_032621]	2.34
STK33	Homo sapiens serine/threonine kinase 33 (STK33), mRNA [NM_030906]	2.34
DHRS2	Homo sapiens dehydrogenase/reductase (SDR family) member 2 (DHRS2), transcript variant 1, mRNA [NM_182908]	2.31
BEX4	Homo sapiens brain expressed, X-linked 4 (BEX4), mRNA [NM_001127688]	2.29

Gene symbol	Description	Fold-change
PAQR7	Homo sapiens progesterin and adipoQ receptor family member VII (PAQR7), mRNA [NM_178422]	2.27
ARC	Homo sapiens activity-regulated cytoskeleton-associated protein (ARC), mRNA [NM_015193]	2.20
SERTAD4	Homo sapiens SERTA domain containing 4 (SERTAD4), mRNA [NM_019605]	2.19
KRT34	Homo sapiens keratin 34 (KRT34), mRNA [NM_021013]	2.13
ARVCF	Homo sapiens armadillo repeat gene deletes in velocardiofacial syndrome (ARVCF), mRNA [NM_001670]	2.12
PSPN	Homo sapiens persephin (PSPN), mRNA [NM_004158]	2.05
EMP1	Homo sapiens epithelial membrane protein 1 (EMP1), mRNA [NM_001423]	1.99
MXD1	Homo sapiens MAX dimerization protein 1 (MXD1), mRNA [NM_002357]	1.98
KLRC3	Homo sapiens killer cell lectin-like receptor subfamily C, member 3 (KLRC3), transcript variant 2, mRNA [NM_007333]	1.97
SLC30A1	Homo sapiens solute carrier family 30 (zinc transporter), member 1 (SLC30A1), mRNA [NM_021194]	1.96
DUSP8	Homo sapiens dual specificity phosphatase 8 (DUSP8), mRNA [NM_004420]	1.92
MMP1	Homo sapiens matrix metalloproteinase 1 (interstitial collagenase) (MMP1), mRNA [NM_002421]	1.91
LOC221710	Homo sapiens hypothetical protein LOC221710 (LOC221710), mRNA [NM_001135575]	1.90
SLCO4A1	Homo sapiens solute carrier organic anion transporter family, member 4A1 (SLCO4A1), mRNA [NM_016354]	1.88
NPL	Homo sapiens N-acetylneuraminic acid pyruvate lyase (dihydrodipicolinate synthase) (NPL), mRNA [NM_030769]	1.84
SLFN5	Homo sapiens schlafen family member 5 (SLFN5), mRNA [NM_144975]	1.82
KLRC1	Homo sapiens killer cell lectin-like receptor subfamily C, member 1 (KLRC1), transcript variant 1, mRNA [NM_002259]	1.80
RFPL2	Homo sapiens ret finger protein-like 2 (RFPL2), transcript variant 1, mRNA [NM_006605]	1.78
CAMTA1	Homo sapiens calmodulin binding transcription activator 1 (CAMTA1), mRNA [NM_015215]	1.77
FOSB	Homo sapiens FBJ murine osteosarcoma viral oncogene homolog B (FOSB), transcript variant 1, mRNA [NM_006732]	1.77
LOC100129113	Homo sapiens cDNA FLJ37158 fis, clone BRACE2026293. [AK094477]	1.77

Gene symbol	Description	Fold-change
KLRC2	Homo sapiens killer cell lectin-like receptor subfamily C, member 2 (KLRC2), mRNA [NM_002260]	1.77
ZNF365	Homo sapiens zinc finger protein 365 (ZNF365), transcript variant A, mRNA [NM_014951]	1.76
ENG	Homo sapiens endoglin (ENG), transcript variant 2, mRNA [NM_000118]	1.74
CCNG2	Homo sapiens cyclin G2 (CCNG2), mRNA [NM_004354]	1.73
IL11	Homo sapiens interleukin 11 (IL11), mRNA [NM_000641]	1.73
MYBL1	Homo sapiens v-myb myeloblastosis viral oncogene homolog (avian)-like 1 (MYBL1), mRNA [NM_001080416]	1.71
C17orf67	Homo sapiens chromosome 17 open reading frame 67 (C17orf67), mRNA [NM_001085430]	1.71
NEFL	Homo sapiens neurofilament, light polypeptide (NEFL), mRNA [NM_006158]	1.67
DNER	Homo sapiens delta/notch-like EGF repeat containing (DNER), mRNA [NM_139072]	1.66
MT1JP	Homo sapiens MTB (MTB) mRNA, complete cds. [AF348994]	1.66
TMEM158	Homo sapiens transmembrane protein 158 (TMEM158), mRNA [NM_015444]	1.64
RGS16	Homo sapiens regulator of G-protein signaling 16 (RGS16), mRNA [NM_002928]	1.64
NEK7	Homo sapiens NIMA (never in mitosis gene a)-related kinase 7 (NEK7), mRNA [NM_133494]	1.62
CCNG2	Homo sapiens cyclin G2 (CCNG2), mRNA [NM_004354]	1.61
BARHL1	Homo sapiens BarH-like homeobox 1 (BARHL1), mRNA [NM_020064]	1.60
FAM129A	Homo sapiens family with sequence similarity 129, member A (FAM129A), transcript variant 2, mRNA [NM_052966]	1.59
CCL20	Homo sapiens chemokine (C-C motif) ligand 20 (CCL20), transcript variant 1, mRNA [NM_004591]	1.59
GEM	Homo sapiens GTP binding protein overexpressed in skeletal muscle (GEM), transcript variant 1, mRNA [NM_005261]	1.58
PAIP2B	Homo sapiens poly(A) binding protein interacting protein 2B (PAIP2B), mRNA [NM_020459]	1.58
G0S2	Homo sapiens G0/G1 switch 2 (G0S2), mRNA [NM_015714]	1.57
HIDAC9	Homo sapiens histone deacetylase 9 (HIDAC9), transcript variant 3, mRNA [NM_014707]	1.56
IGF2	Homo sapiens insulin-like growth factor 2 (somatomedin A) (IGF2), transcript variant 1, mRNA [NM_000612]	1.55

Gene symbol	Description	Fold-change
CLDN12	Homo sapiens claudin 12 (CLDN12), mRNA [NM_012129]	1.52
CEP110	Homo sapiens centrosomal protein 110kDa (CEP110), mRNA [NM_007018]	1.50
FLJ35024	Homo sapiens hypothetical LOC401491 (FLJ35024), non-coding RNA [NR_015375]	1.49
MCL1	Homo sapiens myeloid cell leukemia sequence 1 (BCL2-related) (MCL1), transcript variant 1, mRNA [NM_021960]	1.46
HMOX1	Homo sapiens heme oxygenase (decycling) 1 (HMOX1), mRNA [NM_002133]	1.46
KLRC4	Homo sapiens killer cell lectin-like receptor subfamily C, member 4 (KLRC4), mRNA [NM_013431]	1.45
TMEM139	Homo sapiens transmembrane protein 139 (TMEM139), mRNA [NM_153345]	1.45
H19	Homo sapiens H19, imprinted maternally expressed transcript (non-protein coding) (H19), non-coding RNA [NR_002196]	1.45
ZNF165	Homo sapiens zinc finger protein 165 (ZNF165), mRNA [NM_003447]	1.43
HSPA1A	Homo sapiens heat shock 70kDa protein 1A (HSPA1A), mRNA [NM_005345]	1.43
MAFB	Homo sapiens v-maf musculoaponeurotic fibrosarcoma oncogene homolog B (avian) (MAFB), mRNA [NM_005461]	1.42
PNPLA8	Homo sapiens patatin-like phospholipase domain containing 8 (PNPLA8), mRNA [NM_015723]	1.41
C5orf41	Homo sapiens chromosome 5 open reading frame 41 (C5orf41), mRNA [NM_153607]	1.41
LOC643201	Homo sapiens cDNA clone IMAGE:5268504. [BC052945]	1.40
ARMETL1	Homo sapiens arginine-rich, mutated in early stage tumors-like 1 (ARMETL1), mRNA [NM_001029954]	1.40
WDR69	Homo sapiens WD repeat domain 69 (WDR69), mRNA [NM_178821]	1.37
DDIT3	Homo sapiens DNA-damage-inducible transcript 3 (DDIT3), mRNA [NM_004083]	1.35
FOS	Homo sapiens v-fos FBJ murine osteosarcoma viral oncogene homolog (FOS), mRNA [NM_005252]	1.32
ARL5B	Homo sapiens ADP-ribosylation factor-like 5B (ARL5B), mRNA [NM_178815]	1.32
JUN	Homo sapiens jun oncogene (JUN), mRNA [NM_002228]	1.32
ERRFI1	Homo sapiens ERBB receptor feedback inhibitor 1 (ERRFI1), mRNA [NM_018948]	1.31
CCT6B	Homo sapiens chaperonin containing TCP1, subunit 6B (zeta 2) (CCT6B), mRNA [NM_006584]	1.31
TPPP3	Homo sapiens tubulin polymerization-promoting protein family member 3 (TPPP3), mRNA [NM_016140]	1.30

Gene symbol	Description	Fold-change
PPP2R5C	Homo sapiens mRNA; cDNA DKFZp761H0317 (from clone DKFZp761H0317). [AL834350]	1.30
HRK	Homo sapiens harakiri, BCL2 interacting protein (contains only BH3 domain) (HRK), mRNA [NM_003806]	1.27
MALAT1	Homo sapiens metastasis associated lung adenocarcinoma transcript 1 (non-protein coding) (MALAT1), non-coding RNA [NR_002819]	1.27
C4orf16	Homo sapiens chromosome 4 open reading frame 16 (C4orf16), transcript variant 1, mRNA [NM_018569]	1.27
FES	Homo sapiens feline sarcoma oncogene (FES), transcript variant 1, mRNA [NM_002005]	1.27
SDR42E1	Homo sapiens short chain dehydrogenase/reductase family 42E, member 1 (SDR42E1), mRNA [NM_145168]	1.26
LY6K	Homo sapiens lymphocyte antigen 6 complex, locus K (LY6K), mRNA [NM_017527]	1.26
KLHL24	Homo sapiens kelch-like 24 (Drosophila) (KLHL24), mRNA [NM_017644]	1.26
TMEM50B	Homo sapiens transmembrane protein 50B (TMEM50B), mRNA [NM_006134]	1.25
EREG	Homo sapiens epiregulin (EREG), mRNA [NM_001432]	1.25
HK2	Homo sapiens hexokinase 2 (HK2), mRNA [NM_000189]	1.24
RBAK	Homo sapiens RB-associated KRAB zinc finger (RBAK), mRNA [NM_021163]	1.23
RNF6	Homo sapiens ring finger protein (C3H2C3 type) 6 (RNF6), transcript variant 1, mRNA [NM_005977]	1.23
CCL26	Homo sapiens chemokine (C-C motif) ligand 26 (CCL26), mRNA [NM_006072]	1.21
TP53NP1	Homo sapiens tumor protein p53 inducible nuclear protein 1 (TP53NP1), transcript variant 1, mRNA [NM_033285]	1.21
STXBP6	Homo sapiens syntaxin binding protein 6 (amisyn) (STXBP6), mRNA [NM_014178]	1.21
GCAT	Homo sapiens glycine C-acetyltransferase (2-amino-3-ketobutyrate coenzyme A ligase) (GCAT), nuclear gene encoding mitochondrial protein, mRNA [NM_014291]	1.21
SLC2A3P1	Human glucose transporter pseudogene. [M55536]	1.21
ZNF765	Homo sapiens zinc finger protein 765 (ZNF765), mRNA [NM_001040185]	1.20
CHST2	Homo sapiens carbohydrate (N-acetylglucosamine-6-O) sulfotransferase 2 (CHST2), mRNA [NM_004267]	1.20
SH3YL1	Homo sapiens SH3 domain containing, Ysc84-like 1 (S. cerevisiae) (SH3YL1), mRNA [NM_015677]	1.20

Gene symbol	Description	Fold-change
STX16	Homo sapiens syntaxin 16 (STX16), transcript variant 1, mRNA [NM_001001433]	1.20
ZNF425	Homo sapiens zinc finger protein 425 (ZNF425), mRNA [NM_001001661]	1.19
GPRC5A	Homo sapiens G protein-coupled receptor, family C, group 5, member A (GPRC5A), mRNA [NM_003979]	1.19
MEX3B	Homo sapiens mex-3 homolog B (C. elegans) (MEX3B), mRNA [NM_032246]	1.18
SCML1	Homo sapiens sex comb on midleg-like 1 (Drosophila) (SCML1), transcript variant 1, mRNA [NM_001037540]	1.18
ZNF22	Homo sapiens zinc finger protein 22 (KOX 15) (ZNF22), mRNA [NM_006963]	1.18
ALDOA	Homo sapiens aldolase A, fructose-bisphosphate (ALDOA), transcript variant 2, mRNA [NM_184041]	1.17
SLC22A4	Homo sapiens solute carrier family 22 (organic cation/ergothioneine transporter), member 4 (SLC22A4), mRNA [NM_003059]	1.16
ZNF181	Homo sapiens zinc finger protein 181 (ZNF181), mRNA [NM_001029997]	1.16
LOC728537	Homo sapiens cDNA clone IMAGE:5271446. [BC039374]	1.16
USP36	Homo sapiens cDNA FLJ12851 fis, clone NT2RP2003401, weakly similar to UBIQUITIN CARBOXYL-TERMINAL HYDROLASE DUB-1 (EC 3.1.2.15). [AK022913]	1.15
ZNF600	Homo sapiens zinc finger protein 600 (ZNF600), mRNA [NM_198457]	1.15
SLC6A15	Homo sapiens solute carrier family 6 (neutral amino acid transporter), member 15 (SLC6A15), transcript variant 1, mRNA [NM_182767]	1.15
FBXL19	Homo sapiens F-box and leucine-rich repeat protein 19 (FBXL19), mRNA [NM_001099784]	1.15
CSF2RA	Homo sapiens colony stimulating factor 2 receptor, alpha, low-affinity (granulocyte-macrophage) (CSF2RA), transcript variant 6, mRNA [NM_172249]	1.14
SERP1	Homo sapiens stress-associated endoplasmic reticulum protein 1 (SERP1), mRNA [NM_014445]	1.14
NANOS1	Homo sapiens nanos homolog 1 (Drosophila) (NANOS1), mRNA [NM_199461]	1.13
LOC10013106	Homo sapiens cDNA FLJ38695 fis, clone KIDNE2001897. [AK096014]	1.13
7		
RIMS3	Homo sapiens regulating synaptic membrane exocytosis 3 (RIMS3), mRNA [NM_014747]	1.13
ZNF669	Homo sapiens zinc finger protein 669 (ZNF669), transcript variant 1, mRNA [NM_024804]	1.12

Gene symbol	Description	Fold-change
CD22	Homo sapiens cDNA: FLJ22814 fis, clone KAJA3004. [AK026467]	1.12
NOV	Homo sapiens nephroblastoma overexpressed gene (NOV), mRNA [NM_002514]	1.12
ZNF554	Homo sapiens zinc finger protein 554 (ZNF554), mRNA [NM_001102651]	1.12
C5orf13	Homo sapiens chromosome 5 open reading frame 13 (C5orf13), transcript variant 1, mRNA [NM_004772]	1.11
YOD1	Homo sapiens YOD1 OTU deubiquitinating enzyme 1 homolog (S. cerevisiae) (YOD1), mRNA [NM_018566]	1.11
IL23A	Homo sapiens interleukin 23, alpha subunit p19 (IL23A), mRNA [NM_016584]	1.11
FAM49A	Homo sapiens family with sequence similarity 49, member A (FAM49A), mRNA [NM_030797]	1.10
ZNF606	Homo sapiens zinc finger protein 606 (ZNF606), mRNA [NM_025027]	1.10
NCRNA00084	Homo sapiens non-protein coding RNA 84 (NCRNA00084), non-coding RNA [NR_002802]	1.10
ZMYND12	Homo sapiens zinc finger, MYND-type containing 12 (ZMYND12), mRNA [NM_032257]	1.10
ZNF596	Homo sapiens zinc finger protein 596 (ZNF596), transcript variant 1, mRNA [NM_001042416]	1.10
DNAJB9	Homo sapiens DnaJ (Hsp40) homolog, subfamily B, member 9 (DNAJB9), mRNA [NM_012328]	1.10
TRIM36	Homo sapiens tripartite motif-containing 36 (TRIM36), transcript variant 1, mRNA [NM_018700]	1.10
BAT4	Homo sapiens HLA-B associated transcript 4 (BAT4), mRNA [NM_033177]	1.10
AKAP12	Homo sapiens A kinase (PRKA) anchor protein 12 (AKAP12), transcript variant 2, mRNA [NM_144497]	1.10
RCOR1	Homo sapiens REST corepressor 1 (RCOR1), mRNA [NM_015156]	1.09
ZNF761	Homo sapiens zinc finger protein 761 (ZNF761), mRNA [NM_001008401]	1.09
RNF138	Homo sapiens ring finger protein 138 (RNF138), transcript variant 1, mRNA [NM_016271]	1.08
SLAMF7	Homo sapiens SLAM family member 7 (SLAMF7), mRNA [NM_021181]	1.08
SNX25	Homo sapiens sorting nexin 25 (SNX25), mRNA [NM_031953]	1.08
FYN	Homo sapiens FYN oncogene related to SRC, FGR, YES (FYN), transcript variant 1, mRNA [NM_002037]	1.08

ene symbol	Description	Fold-change
DRB2	Homo sapiens adrenergic, beta-2-, receptor, surface (ADRB2), mRNA [NM_000024]	1.08
SP5	Homo sapiens dual specificity phosphatase 5 (DUSP5), mRNA [NM_004419]	1.08
RA3	Homo sapiens HtrA serine peptidase 3 (HTRA3), mRNA [NM_053044]	1.08
EKHA4	Homo sapiens pleckstrin homology domain containing, family A (phosphoinositide binding specific) member 4 (PLEKHA4), mRNA [NM_020904]	1.07
PI2	Homo sapiens tissue factor pathway inhibitor 2 (TFPI2), mRNA [NM_006528]	1.07
ADD3	Homo sapiens adducin 3 (gamma) (ADD3), transcript variant 1, mRNA [NM_016824]	1.07
MBNL2	Homo sapiens muscleblind-like 2 (Drosophila) (MBNL2), transcript variant 1, mRNA [NM_144778]	1.07
CITED2	Homo sapiens Cbp/p300-interacting transactivator, with Glu/Asp-rich carboxy-terminal domain, 2 (CITED2), mRNA [NM_006079]	1.07
CS2	Homo sapiens suppressor of cytokine signaling 2 (SOCS2), mRNA [NM_003877]	1.07
F664	Homo sapiens zinc finger protein 664 (ZNF664), mRNA [NM_152437]	1.06
CXCR4	Homo sapiens chemokine (C-X-C motif) receptor 4 (CXCR4), transcript variant 1, mRNA [NM_001008540]	1.06
4-Mar	Homo sapiens membrane-associated ring finger (C3HC4) 4 (MARCH4), mRNA [NM_020814]	1.06
L26	Homo sapiens chemokine (C-C motif) ligand 26 (CCL26), mRNA [NM_006072]	1.06
1orf91	Homo sapiens chromosome 21 open reading frame 91 (C21orf91), transcript variant 2, mRNA [NM_017447]	1.06
NE1	Homo sapiens spectrin repeat containing, nuclear envelope 1 (SYNE1), transcript variant 2, mRNA [NM_033071]	1.05
ANXA1	Homo sapiens sperm protein associated with the nucleus, X-linked, family member A1 (SPANXA1), mRNA [NM_013453]	1.05
DN	Homo sapiens pallidin homolog (mouse) (PLDN), mRNA [NM_012388]	1.05
RC58	Homo sapiens leucine rich repeat containing 58 (LRRCS8), mRNA [NM_001099678]	1.05
ARID5B	Homo sapiens AT rich interactive domain 5B (MRF1-like) (ARID5B), mRNA [NM_032199]	1.04

Gene symbol	Description	Fold-change
LOC643401	Homo sapiens hypothetical protein LOC340109, mRNA (cDNA clone IMAGE:5578073), partial cds. [BC039509]	1.04
WBP5	Homo sapiens WW domain binding protein 5 (WBP5), transcript variant 1, mRNA [NM_016303]	1.04
TRIB1	Homo sapiens tribbles homolog 1 (Drosophila) (TRIB1), mRNA [NM_025195]	1.04
NTSE	Homo sapiens 5'-nucleotidase, ecto (CD73) (NTSE), mRNA [NM_002526]	1.04
DMBT1	Homo sapiens deleted in malignant brain tumors 1 (DMBT1), transcript variant 2, mRNA [NM_007329]	1.04
PAG1	Homo sapiens phosphoprotein associated with glycosphingolipid microdomains 1 (PAG1), mRNA [NM_018440]	1.04
PTPRH	Homo sapiens protein tyrosine phosphatase, receptor type, H (PTPRH), mRNA [NM_002842]	1.04
CSTA	Homo sapiens cystatin A (stefin A) (CSTA), mRNA [NM_005213]	1.04
LOC100130288	Homo sapiens cDNA clone IMAGE:5295205, with apparent retained intron. [BC043212]	1.04
THAP5	Homo sapiens THAP domain containing 5 (THAP5), transcript variant 2, mRNA [NM_182529]	1.04
DHDH	Homo sapiens dihydrodiol dehydrogenase (dimeric) (DHDH), mRNA [NM_014475]	1.03
TPD52	Homo sapiens tumor protein D52 (TPD52), transcript variant 1, mRNA [NM_001025252]	1.03
SPOCD1	Homo sapiens cDNA FLJ39908 fis, clone SPLEN2017620. [AK097227]	1.03
C1orf133	Homo sapiens chromosome 1 open reading frame 133 (C1orf133), non-coding RNA [NR_024337]	1.03
NR4A1	Homo sapiens nuclear receptor subfamily 4, group A, member 1 (NR4A1), transcript variant 1, mRNA [NM_002135]	1.03
ZNF302	Homo sapiens zinc finger protein 302 (ZNF302), transcript variant 1, mRNA [NM_018443]	1.03
KLHL23	Homo sapiens kelch-like 23 (Drosophila) (KLHL23), mRNA [NM_144711]	1.03
AADAC	Homo sapiens arylacetamide deacetylase (esterase) (AADAC), mRNA [NM_001086]	1.02
GAS5	Homo sapiens growth arrest-specific 5 (non-protein coding) (GAS5), non-coding RNA [NR_002578]	1.02

Gene symbol	Description	Fold-change
C17orf91	Homo sapiens chromosome 17 open reading frame 91 (C17orf91), transcript variant 1, mRNA [NM_032895]	1.02
CYP1A1	Homo sapiens cytochrome P450, family 1, subfamily A, polypeptide 1 (CYP1A1), mRNA [NM_000499]	1.02
LYPD6	Homo sapiens LY6/PLAUR domain containing 6 (LYPD6), mRNA [NM_194317]	1.02
MBNL1	Homo sapiens muscleblind-like (Drosophila) (MBNL1), transcript variant 6, mRNA [NM_207296]	1.02
LOC100133236	PREDICTED: Homo sapiens hypothetical protein LOC100133236 (LOC100133236), mRNA [XM_001714262]	1.02
6	Homo sapiens BCL2/adenovirus E1B 19kDa interacting protein 3-like (BNIP3L), mRNA [NM_004331]	1.02
BNIP3L	Homo sapiens BCL2/adenovirus E1B 19kDa interacting protein 3-like (BNIP3L), mRNA [NM_004331]	1.02
ST7OT1	Homo sapiens ST7 overlapping transcript 1 (non-protein coding) (ST7OT1), non-coding RNA [NR_002330]	1.02
SPANXD	Homo sapiens SPANX family, member D (SPANXD), mRNA [NM_032417]	1.02
FBXO32	Homo sapiens F-box protein 32 (FBXO32), transcript variant 1, mRNA [NM_058229]	1.02
C6orf199	Homo sapiens chromosome 6 open reading frame 199 (C6orf199), mRNA [NM_145025]	1.02
SGMS2	Homo sapiens sphingomyelin synthase 2 (SGMS2), transcript variant 1, mRNA [NM_152621]	1.02
PLAG1	Homo sapiens pleiomorphic adenoma gene 1 (PLAG1), transcript variant 1, mRNA [NM_002655]	1.01
ZNF808	Homo sapiens zinc finger protein 808 (ZNF808), mRNA [NM_001039886]	1.01
HSD17B12	Homo sapiens hydroxysteroid (17-beta) dehydrogenase 12 (HSD17B12), mRNA [NM_016142]	1.01
FOSL1	Homo sapiens FOS-like antigen 1 (FOSL1), mRNA [NM_005438]	1.01
ZNF238	Homo sapiens zinc finger protein 238 (ZNF238), transcript variant 2, mRNA [NM_006352]	1.01
RAB3B	Homo sapiens RAB3B, member RAS oncogene family (RAB3B), mRNA [NM_002867]	1.01
PTX3	Homo sapiens pentraxin-related gene, rapidly induced by IL-1 beta (PTX3), mRNA [NM_002852]	1.00

Table S2 List of the Genes Down-regulated by 100 µg / mL of ZnO-NPs in A549 cells.

Gene symbol	Description	Fold-change
KIAA1199	Homo sapiens KIAA1199 (KIAA1199), mRNA [NM_018689]	-2.61
CBLN2	Homo sapiens cerebellin 2 precursor (CBLN2), mRNA [NM_182511]	-1.93
LOC553137	Homo sapiens cDNA FLJ42409 fis, clone BLADE2000866. [AK124400]	-1.86
SLC39A10	Homo sapiens solute carrier family 39 (zinc transporter), member 10 (SLC39A10), transcript variant 2, mRNA [NM_020342]	-1.79
BAAT	Homo sapiens bile acid Coenzyme A: amino acid N-acyltransferase (glycine N-choloyltransferase) (BAAT), transcript variant 1, mRNA [NM_001701]	-1.77
CPLX2	Homo sapiens complexin 2 (CPLX2), transcript variant 1, mRNA [NM_006650]	-1.74
TMEM37	Homo sapiens transmembrane protein 37 (TMEM37), mRNA [NM_183240]	-1.68
HLA-DMB	Homo sapiens major histocompatibility complex, class II, DM beta (HLA-DMB), mRNA [NM_002118]	-1.68
LGALS2	Homo sapiens lectin, galactoside-binding, soluble, 2 (LGALS2), mRNA [NM_006498]	-1.67
GPX2	Homo sapiens glutathione peroxidase 2 (gastrointestinal) (GPX2), mRNA [NM_002083]	-1.65
FGG	Homo sapiens fibrinogen gamma chain (FGG), transcript variant gamma-A, mRNA [NM_000509]	-1.63
DACT2	Homo sapiens dapper, antagonist of beta-catenin, homolog 2 (Xenopus laevis) (DACT2), mRNA [NM_214462]	-1.59
SYT13	Homo sapiens synaptotagmin XIII (SYT13), mRNA [NM_020826]	-1.58
C4orf18	Homo sapiens chromosome 4 open reading frame 18 (C4orf18), transcript variant 2, mRNA [NM_016613]	-1.56
OLFML3	Homo sapiens olfactomedin-like 3 (OLFML3), mRNA [NM_020190]	-1.56
VAV3	Homo sapiens vav 3 guanine nucleotide exchange factor (VAV3), transcript variant 1, mRNA [NM_006113]	-1.54
PRICKLE2	Homo sapiens prickly homolog 2 (Drosophila) (PRICKLE2), mRNA [NM_198859]	-1.54
C12orf27	Homo sapiens chromosome 12 open reading frame 27 (C12orf27), non-coding RNA [NR_024345]	-1.53
PLCXD3	Homo sapiens phosphatidylinositol-specific phospholipase C, X domain containing 3 (PLCXD3), mRNA [NM_001005473]	-1.48

Gene symbol	Description	Fold-change
PLA2G4A	Homo sapiens phospholipase A2, group IVA (cytosolic, calcium-dependent) (PLA2G4A), mRNA [NM_024420]	-1.46
GRIK2	Homo sapiens glutamate receptor, ionotropic, kainate 2 (GRIK2), transcript variant 2, mRNA [NM_175768]	-1.46
CCL2	Homo sapiens chemokine (C-C motif) ligand 2 (CCL2), mRNA [NM_002982]	-1.44
IFIT1	Homo sapiens interferon-induced protein with tetratricopeptide repeats 1 (IFIT1), transcript variant 2, mRNA [NM_001548]	-1.42
CORO2A	Homo sapiens coronin, actin binding protein, 2A (CORO2A), transcript variant 1, mRNA [NM_003389]	-1.42
ASGR1	Homo sapiens asialoglycoprotein receptor 1 (ASGR1), mRNA [NM_001671]	-1.41
CD24	Homo sapiens CD24 signal transducer mRNA, complete cds and 3' region. [L33930]	-1.38
SFRP4	Homo sapiens secreted frizzled-related protein 4 (SFRP4), mRNA [NM_003014]	-1.38
INSL4	Homo sapiens insulin-like 4 (placenta) (INSL4), mRNA [NM_002195]	-1.36
CLDN2	Homo sapiens claudin 2 (CLDN2), mRNA [NM_020384]	-1.35
SULT2B1	Homo sapiens sulfotransferase family, cytosolic, 2B, member 1 (SULT2B1), transcript variant 1, mRNA [NM_004605]	-1.34
USH1C	Homo sapiens Usher syndrome 1C (autosomal recessive, severe) (USH1C), transcript variant 1, mRNA [NM_005709]	-1.33
CP	Homo sapiens ceruloplasmin (ferroxidase) (CP), mRNA [NM_000096]	-1.32
MUC5AC	Homo sapiens mucin 5AC, oligomeric mucus/gel-forming (MUC5AC), mRNA [NM_017511]	-1.32
CDH1	Homo sapiens cadherin 1, type 1, E-cadherin (epithelial) (CDH1), mRNA [NM_004360]	-1.31
TC2N	Homo sapiens tandem C2 domains, nuclear (TC2N), transcript variant 1, mRNA [NM_152332]	-1.31
PHYHIP1L	Homo sapiens phytanoyl-CoA 2-hydroxylase interacting protein-like (PHYHIP1L), transcript variant 1, mRNA [NM_032439]	-1.30
NPY1R	Homo sapiens neuropeptide Y receptor Y1 (NPY1R), mRNA [NM_000909]	-1.30
DIRAS3	Homo sapiens DIRAS family, GTP-binding RAS-like 3 (DIRAS3), mRNA [NM_004675]	-1.30
DEFB1	Homo sapiens defensin, beta 1 (DEFB1), mRNA [NM_005218]	-1.29

Gene symbol	Description	Fold-change
ELMO1	Homo sapiens engulfment and cell motility 1 (ELMO1), transcript variant 1, mRNA [NM_014800]	-1.29
RNF43	Homo sapiens ring finger protein 43 (RNF43), mRNA [NM_017763]	-1.28
AKR1C3	Homo sapiens aldo-keto reductase family 1, member C3 (3-alpha hydroxysteroid dehydrogenase, type II) (AKR1C3), mRNA [NM_003739]	-1.27
OLFML2A	Homo sapiens olfactomedin-like 2A (OLFML2A), mRNA [NM_182487]	-1.27
BTBD11	Homo sapiens BTB (POZ) domain containing 11 (BTBD11), transcript variant a, mRNA [NM_001018072]	-1.26
A1CF	Homo sapiens APOBEC1 complementation factor (A1CF), transcript variant 3, mRNA [NM_138933]	-1.26
HS3ST3B1	Heparan sulfate glucosaminyl 3-O-sulfotransferase 3B1 (EC 2.8.2.30)(Heparan sulfate D-glucosaminyl 3-O-sulfotransferase 3B1)(Heparan sulfate 3-O-sulfotransferase 3B1)(h3-OST-3B) [Source:UniProtKB/Swiss-Prot,Acc:Q9Y662] [ENST00000360954]	-1.26
CFH	Homo sapiens complement factor H (CFH), transcript variant 1, mRNA [NM_000186]	-1.25
C5	Homo sapiens complement component 5 (C5), mRNA [NM_001735]	-1.25
SGK493	Homo sapiens protein kinase-like protein Sgk493 (SGK493), mRNA [NM_138370]	-1.25
LOC554207	Homo sapiens hypothetical LOC554207, mRNA (cDNA clone MGC:21504 IMAGE:3882600, complete cds. [BC031469])	-1.25
IGSF11	Homo sapiens immunoglobulin superfamily, member 11 (IGSF11), transcript variant 1, mRNA [NM_152538]	-1.24
NOSTRIN	Homo sapiens nitric oxide synthase trafficker (NOSTRIN), transcript variant 1, mRNA [NM_052946]	-1.24
NTRK3	Homo sapiens neurotrophic tyrosine kinase, receptor, type 3 (NTRK3), transcript variant 2, mRNA [NM_002530]	-1.24
NPNT	Homo sapiens nephronectin (NPNT), mRNA [NM_001033047]	-1.23
ADAMTS9	Homo sapiens ADAM metalloproteinase with thrombospondin type 1 motif, 9 (ADAMTS9), mRNA [NM_182920]	-1.23
HHIPL2	Homo sapiens HHIP-like 2 (HHIPL2), mRNA [NM_024746]	-1.23
TM4SF20	Homo sapiens transmembrane 4 L six family member 20 (TM4SF20), mRNA [NM_024795]	-1.21
VIL1	Homo sapiens villin 1 (VIL1), mRNA [NM_007127]	-1.20

Gene symbol	Description	Fold-change
RHOV	Homo sapiens ras homolog gene family, member V (RHOV), mRNA [NM_133639]	-1.20
SLC23A1	Homo sapiens solute carrier family 23 (nucleobase transporters), member 1 (SLC23A1), transcript variant 2, mRNA [NM_152685]	-1.20
NR1H4	Homo sapiens nuclear receptor subfamily 1, group H, member 4 (NR1H4), mRNA [NM_005123]	-1.20
NPY5R	Homo sapiens neuropeptide Y receptor Y5 (NPY5R), mRNA [NM_006174]	-1.18
FGB	Homo sapiens fibrinogen beta chain (FGB), mRNA [NM_005141]	-1.17
KCNV1	Homo sapiens potassium channel, subfamily V, member 1 (KCNV1), mRNA [NM_014379]	-1.17
STYK1	Homo sapiens serine/threonine/tyrosine kinase 1 (STYK1), mRNA [NM_018423]	-1.16
FAM171B	Homo sapiens mRNA for KIAA1946 protein. [AB075826]	-1.16
CYP4F3	Homo sapiens mRNA for leukotriene B4 omega-hydroxylase, complete cds. [AB002454]	-1.14
UGT1A6	Homo sapiens UDP glucuronosyltransferase 1 family, polypeptide A6 (UGT1A6), transcript variant 1, mRNA [NM_001072]	-1.14
ST8SIA4	Homo sapiens ST8 alpha-N-acetyl-neuraminide alpha-2,8-sialyltransferase 4 (ST8SIA4), transcript variant 1, mRNA [NM_005668]	-1.13
ATP8B3	Homo sapiens ATPase, class 1, type 8B, member 3 (ATP8B3), mRNA [NM_138813]	-1.13
EPCAM	Homo sapiens epithelial cell adhesion molecule (EPCAM), mRNA [NM_002354]	-1.13
ITIH2	Homo sapiens inter-alpha (globulin) inhibitor I2 (ITIH2), mRNA [NM_002216]	-1.13
DKK1	Homo sapiens dickkopf homolog 1 (Xenopus laevis) (DKK1), mRNA [NM_012242]	-1.12
ZNRF3	Homo sapiens zinc and ring finger 3 (ZNRF3), mRNA [NM_032173]	-1.11
hCG_1776007	Homo sapiens hexaribonucleotide binding protein 3 (HRNBP3), mRNA [NM_001082575]	-1.11
MYO10	Homo sapiens myosin X (MYO10), mRNA [NM_012334]	-1.11
CFI	Homo sapiens complement factor I (CFI), mRNA [NM_000204]	-1.10
KIF13A	Homo sapiens kinesin family member 13A (KIF13A), transcript variant 1, mRNA [NM_022113]	-1.10
GPRC5B	Homo sapiens G protein-coupled receptor, family C, group 5, member B (GPRC5B), mRNA [NM_016235]	-1.09
SLC7A7	Homo sapiens solute carrier family 7 (cationic amino acid transporter, y+ system), member 7 (SLC7A7), transcript variant 1, mRNA [NM_003982]	-1.09
FAM83A	Homo sapiens family with sequence similarity 83, member A (FAM83A), transcript variant 2, mRNA [NM_207006]	-1.09
AKR1C1	Homo sapiens aldo-keto reductase family 1, member C1 (dihydrodiol dehydrogenase 1; 20-alpha (3-alpha)-hydroxysteroid dehydrogenase) (AKR1C1), mRNA [NM_001353]	-1.09